AGU PUBLICATIONS

Geophysical Research Letters

RESEARCH LETTER
10.1002/2014GL061413

Key Points:
- The Dansgaard-Oeschger oscillation is explained using a coupled model
- Mechanism involves a salt oscillator of relaxation oscillator form
- The bipolar seesaw in surface air temperature is accurately predicted

Supporting Information:
- Readme
- Figures S1–S3

Correspondence to:
W. R. Peltier,
peltier@atmosp.physics.utoronto.ca

Citation:
Peltier, W. R., and G. Vettoretti (2014), Dansgaard-Oeschger oscillations predicted in a comprehensive model of glacial climate: A "kicked" salt oscillator in the Atlantic, *Geophys. Res. Lett.*, *41*, doi:10.1002/2014GL061413.

Received 2 AUG 2014
Accepted 30 SEP 2014
Accepted article online 2 OCT 2014

Dansgaard-Oeschger oscillations predicted in a comprehensive model of glacial climate: A "kicked" salt oscillator in the Atlantic

W. Richard Peltier[1] and Guido Vettoretti[1]

[1]Department of Physics, University of Toronto, Toronto, Ontario, Canada

Abstract During the period from 60,000 to 35,000 years ago, Summit-Greenland ice core records of the oxygen isotopic ratio $^{18}O/^{16}O$ exhibit intense millennium time scale oscillations. These Dansgaard-Oeschger oscillations have been interpreted to represent the variations in North Atlantic air temperature caused by correlative changes in the strength of North Atlantic Deep Water production. We apply a comprehensive model of glacial climate to unambiguously identify the mechanism responsible for this phenomenon. This is shown to involve a salt oscillation of relaxation oscillator form. This nonlinear oscillation does not require the existence of feedback due to freshwater release from grounded ice on the continents during the warm phase of the cycle.

1. Introduction

Even though the Dansgaard-Oeschger (D-O) oscillation phenomenon was first discovered 30 years ago [*Dansgaard et al*., 1984, 1993], its mechanistic origins have remained enigmatic. Figure 1a displays the oxygen isotopic ratio time series $\delta^{18}O$ for the North Greenland Ice Core Project (NGRIP) ice core record from Summit, Greenland, where it is compared with several other full glacial cycle records of climate system variability. Numerous mechanisms for this millennial time scale mode of variability, shown expanded in Figure 1b during the Marine Oxygen Isotope Stage 3 (MOIS 3) period, have been suggested. These have included a mechanism derivative of a significant reduction in the strength of the process of deep water formation [e.g., *Sakai and Peltier*, 1996, 1997] subsequent to which the overturning circulation "fibrillates" on the millennium time scale. An alternative hypothesis involves the idea of "stochastic resonance" [*Alley et al*., 2001; *Ganopolski and Rahmstorf*, 2002] in which a small-amplitude harmonic excitation of the Atlantic meridional overturning circulation (AMOC) is amplified in the presence of noise. An even more recent model is one which does not specifically invoke oscillatory variability of the AMOC at all [*Singh et al*., 2014]. A further suggested mechanism is that involving a "salt oscillator" [*Broecker et al*., 1990; *Birchfield and Broecker*, 1990], but this suggestion was advanced on qualitative grounds or in terms of a box model representation which specifically envisioned freshwater forcing as being required. Perhaps the most apparent characteristic of the D-O oscillations during MIOS3 in the NGRIP record of *Andersen et al*. [2004] in Figure 1b is that they are observed to follow individual Heinrich events [*Heinrich*, 1988; *Hemming*, 2004] and therefore are plausibly triggered by them as in the early suggestion of *Timmermann et al*. [2003].

A serious impediment to unambiguous identification of the mechanism underpinning the D-O oscillation phenomenon is that no modern model of the coupled climate system has ever been shown to naturally produce such oscillatory behavior under glacial climate conditions. All such reconstructions of glacial climate [e.g., *Weber et al*., 2007; *Brady et al*., 2013; *Zhang et al*., 2013] have led their authors to conclude that the state of the glacial ocean was a nonoscillatory quasi-equilibrium in which the strength of the AMOC was either increased or reduced from modern preindustrial climate. The most recent example of such analyses is that by *Vettoretti and Peltier* [2013] who employed the Community Climate System Model version 3 (CCSM3) model to perform an Last Glacial Maximum (LGM) reconstruction at higher spatial resolution than previously employed to suggest that in it, the equilibrium state of the glacial ocean was a stable state in which the strength of the AMOC was reduced by 40–45% from its modern strength. A reduction in strength of this magnitude accords with that based upon the use of the Pa/Th tracer of the kinematic strength of the deep western boundary undercurrent of the North Atlantic Basin [*McManus et al*., 2004].

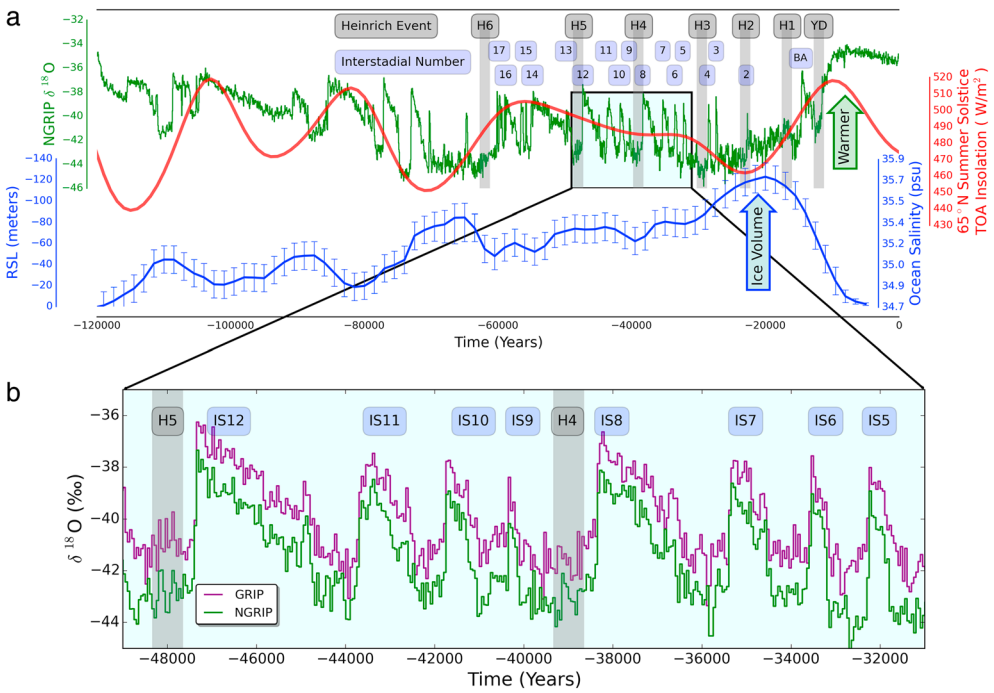

Figure 1. (a) Last glacial cycle time series: NGRIP δ^{18}O (‰) (green) versus 65°N insolation (W m^{-2}) (red) compared with relative sea level (RSL) (meters) (blue) which correlates with changes in ocean salinity (practical salinity units, psu). The RSL history has been inverted to display increasing ice volume and its relationship to increasing ocean salinity. Heinrich events are labeled "H." D-O interstadials are blue. (b) NGRIP (green) and GRIP (purple) δ^{18}O time series (‰) through the indicated subsection of MOIS 3.

2. Dansgaard-Oeschger Oscillations in Community Earth System Model Version 1

In order to test the robustness of these latest results concerning the existence of an apparently stable state of the glacial AMOC, we employ the Community Earth System Model version 1 (CESM1 [*Gent et al.*, 2011]; see the supporting information for the configuration of this model we employ). It has previously been suggested [*Sakai and Peltier*, 2001] that oscillatory behavior in such models might concern the nature of the damping to which the ocean circulation is subject. In the work reported here we investigate the impact of variations in the diapycnal diffusivity "κ" upon the nature of the solutions for glacial climate delivered by CESM1. This parameter is assumed to govern the rate at which the cold salty waters of the abyssal ocean generated by deep water production at the poles are able to "upwell" to close the two deep overturning cells of which the Atlantic MOC is comprised [*Munk*, 1966; *Munk and Wunsch*, 1998]. In our glacial version of the CESM1 model the diapycnal and related momentum diffusivity have been significantly modified from those employed in CESM1. The rationale for this is based upon the fact that the diapycnal diffusivity in CESM1 includes a dominant contribution due to turbulent mixing associated with the breaking of the internal tide generated by the flow of the barotropic tide over ocean bottom topography. On our analyses, we have elected to eliminate this extremely space-dependent and inadequately constrained form of the turbulent diffusivity based upon the fact that it is directly tied to the modern tidal regime. This is known to have differed dramatically under glacial conditions because of the significant changes in bathymetric depth due to the reduction in sea level caused by the growth of ice age ice sheets on the continents [*Griffiths and Peltier*, 2009]. The diapycnal diffusivity map employed in CESM1 is shown in Figure S1 in the supporting information together with the alternative models we will employ.

In our analyses, we have employed several distinct choices for κ as well as the original parameterization based upon tidal mixing (for comparison purposes). The first choice has κ fixed to the background CESM1 pelagic value of 0.17 cm^2/s throughout the ocean volume. The second choice assumes κ to be fixed to the same depth-dependent profile assumed in the POP1 ocean component of the previous CCSM3 version of the NCAR model which has been shown to deliver a nonoscillatory glacial climate state [*Vettoretti and Peltier*,

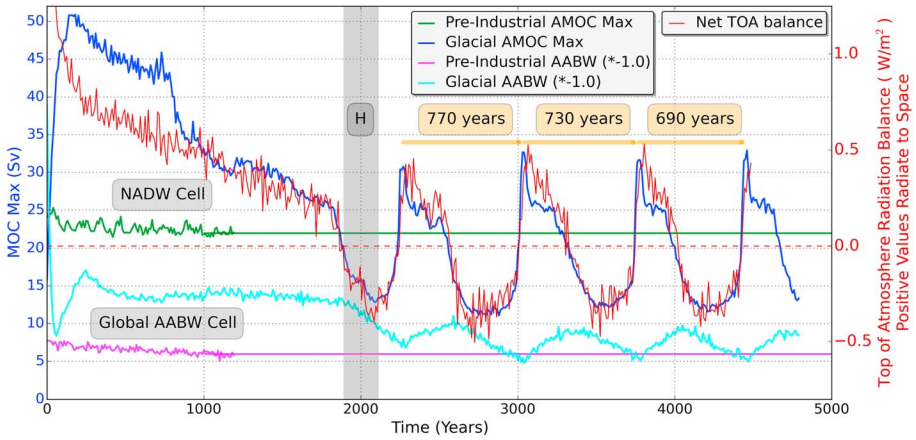

Figure 2. Eulerian mean glacial AMOC maximum (1 Sv = 10^6 m^3/s) (dark blue) compared with glacial top of the atmosphere radiation balance (W/m^2) (red) and global Eulerian mean glacial AABW minimum (−Sv) (blue). The stable preindustrial control simulation (green) has been extended with a horizontal line to enable comparison with the much longer glacial simulation. The periods of the individual D-O cycles are observed to decrease slowly with time.

2013]. Because our analyses will show that the CESM1 model delivers Dansgaard-Oeschger oscillations for both simple representations of diapycnal diffusivity, this will aid in isolating the differences between the ocean components of these models that are apparently responsible for allowing CESM1 to oscillate, whereas CCSM3 does not. Although both of these models of diapycnal diffusivity differ somewhat from the modern observational constraints, these remain extremely sparse (e.g., see *Waterhouse et al*. [2014] for a recent review; Figure S1 provides specific examples).

Our CESM1 simulations of glacial climate employ the recently constructed ICE-6G (VM5a) model of glacial boundary conditions [*Argus et al*., 2014; *Peltier et al*., 2014], a model which is an existing option for use in the context of the Paleoclimate Modeling Intercomparison Project 3 (https://pmip3.lsce.ipsl.fr/). Upon introduction of these boundary conditions into CESM1, we obtain the time series of the evolution of AMOC strength in Sverdrups (1 Sv = 10^6 m^3/s) shown in Figure 2 for both the preindustrial control climate and for the climate of the glacial state. In this first example, we have employed the simplest of the κ models mentioned above. The entire "spin-up" to the final temporally evolving glacial state has required an unprecedented 4500 simulated years of integration of the high-resolution CESM1 model at full CMIP5 resolution (See Table S1 for the details of simulation design). It is notable that the final statistical equilibrium of the glacial AMOC shown on Figure 2 is characterized by an intense oscillation of strength that extends to values both above and below the 22 Sv that is characteristic of the modern preindustrial control climate (The nonoscillatory preindustrial control has employed the same pelagic diapycnal diffusivity as in the glacial simulation). Oscillation strength in the glacial climate regime varies from a minimum near 12.5 Sv to a maximum near 30 Sv. The minimum is 40–45% below the strength of the preindustrial control, approximately the same reduction previously obtained in the CCSM3 analyses [*Vettoretti and Peltier*, 2013]. Notable also is the fact that the period of the AMOC oscillation is in the D-O regime.

We have rerun this LGM integration using the same diffusivity profile as that employed in the POP1 ocean component of the CCSM3 model, and the results are shown in Figure S2. This figure demonstrates that the oscillatory behavior also occurs under these significantly different conditions of diapycnal diffusivity. In this case the period and amplitude of the oscillation are both increased by approximately 15%. On this basis, we may conclude that the absence of oscillatory behavior of glacial climate in CCSM3 is not due to the particular choice for its diapycnal diffusivity profile. Rather, this difference in behavior between CCSM3 and CESM1 is most probably associated with the poor representation of southern ocean dynamics in the former model [*Danabasoglu et al*., 2012]. In particular, *Vettoretti and Peltier* [2013, Figure 2] have shown that the strength of the Antarctic Bottom Water (AABW) cell in CCSM3 is excessive. We cannot, however, rule out the possibility that a significant contributor to the difference may be simply due to the fact that the resolution of the POP1 model of the ocean in CCSM3 is significantly lower than that of the POP2 version in CESM1. In Figure S2, we also show the result obtained when the modern tidal mixing based parameterization is employed even though this is expected to be entirely inappropriate for the glacial ocean.

3. D-O Oscillator Mechanics

Under the applied ice age boundary conditions, the model-predicted AMOC strength becomes an almost perfectly periodic function of time for either of the two simplified models of diapycnal diffusivity. This near precision of periodicity in such a highly nonlinear coupled structure as CESM1 could reasonably be seen as suggesting the action of the Hopf bifurcation [*Marsden and McCracken*, 1976], previously suggested to be the underlying cause of the D-O phenomenon [*Sakai and Peltier*, 1997]. In our model the existence of the approximate limit cycle is in part a consequence of the assumption of invariant continental ice sheet mass. In the design of our numerical experiments, we have specifically eliminated the possibility of feedback associated with an oscillation-induced release of meltwater to the oceans from the continental ice sheets. Figure 1a also shows that during MOIS 3, global sea level, as represented by the inference of *Waelbroeck et al*. [2002], remained relatively stationary implying that such feedback may have been weak. When it is ruled out entirely, we predict an almost periodic D-O oscillation. The Hopf bifurcation hypothesis of its origin must be seen as superficial, however, as it provides no explanation of the physical mechanism(s) involved in the limit cycle behavior. An alternative view of the physics of the D-O oscillations in the model is to view the phenomenon as involving a "kicked" oscillator in which a Heinrich event is seen as providing the "kick" which induces the oscillatory behavior. As is clear on the basis of Figure 1, every D-O oscillation or cluster of such oscillations is preceded by a Heinrich event.

It will also be noted that during the portion of MOIS 3 illustrated on Figure 1b, the individual D-O oscillations appear in clusters following Heinrich events H5 and H4. These clusters, of which only two are evident during MOIS 3, have been referred to as "Bond cycles" following their original recognition [*Bond et al*., 1997; see also *Sakai and Peltier*, 1999]. Each millennium-scale pulse of which an individual Bond cycle is composed consists of a rapid initial increase in strength of the AMOC that is accompanied by a rapid warming of Northern Hemisphere climate. Clear recent evidence that AMOC variability is, in fact, involved in the D-O oscillations of MOIS 3 has been provided [*Dokken et al*., 2013]. One of the most interesting aspects of the D-O oscillation mechanism concerns the shape of the individual pulses. These are of "relaxation oscillation" form [*Van der Pol and Van der Mark*, 1928], as the initial fast time scale deep-convection driven rise of AMOC strength is followed by a slow time scale "relaxation" back toward full glacial conditions. Because the clusters of Heinrich events predicted by the model are not characterized by decreasing amplitude of the individual events as observed in Figure 1, this suggest that the "Q" of the D-O oscillator in CESM1 is too high.

The key to understanding the physics underlying the D-O oscillation is to be found in the buildup and collapse of the meridional salinity gradient between the subtropical gyre of the North Atlantic Ocean and that beneath the sea ice cover to the north. To understand the importance of these salinity variations in our model of glacial climate, we display in Figure 3a a zonally averaged Atlantic meridional salinity section as a temporal average across one cycle of the oscillation, and then in Figures 3b and 3c we show the cross-sectional deviations from this temporal average for both peak stadial and peak interstadial conditions. The results of this analysis lead directly to an interpretation of the D-O oscillation in the model as a salt oscillation. Under cold stadial conditions, the salinity of the subtropical gyre of the North Atlantic is anomalously high and the salinity beneath the sea ice lid to the north is anomalously low in a polar halocline (Figure 3b; e.g., see *Rose et al*. [2013] for such halocline development in a simple aquaplanet model). Under warm interstadial conditions, the meridional gradient of the anomalies is reversed (Figure 3c).

Investigation of the temporal evolution of the salinity field and related ocean dynamical processes enables us to identify the main instability mechanism involved in the D-O oscillation phenomenon. That sea ice variability is tightly coupled to AMOC strength is documented in Figure 3d on which we show, for our sequence of D-O pulses from the low diapycnal diffusivity version of the model, an overlay of the time series of the percentage of the North Atlantic covered by sea ice with the annually averaged AMOC strength which establishes the strong coupling between them. In Figure 3e decadal-averaged AMOC strength is shown together with the northward decadal-averaged heat transport in the North Atlantic at 30°N latitude. The near-perfect correlation of the evolving strength of a D-O pulse with the northward ocean heat flux is expected. As sea ice cover expands (contracts), AMOC strength and northward heat transport decreases (increases).

The most important of these time series results are those shown in Figure 3f which displays the covariations of northward ocean salinity flux at 30°N latitude, surface salinity in the subtropical gyre of the North Atlantic,

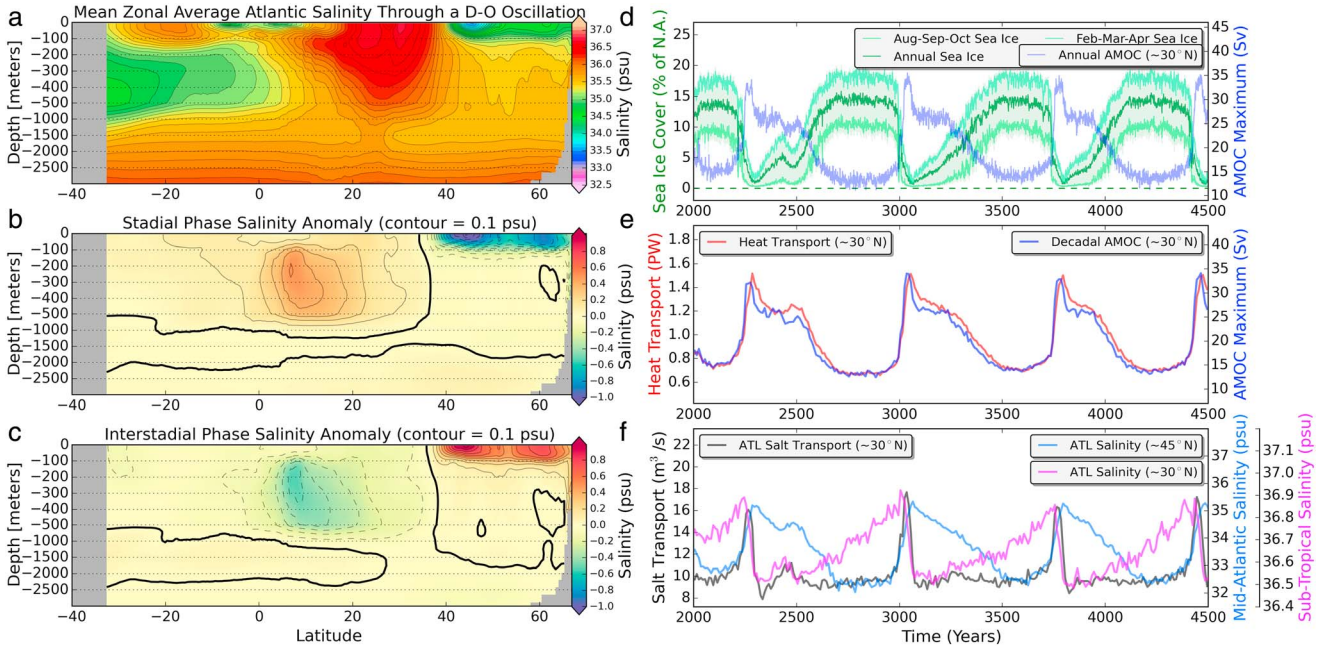

Figure 3. (a) Atlantic D-O cycle zonally and time-averaged salinity of the Atlantic Basin in the low diapycnal diffusivity version of the glacial CESM1 model. (b) Stadial salinity anomaly as the deviation from Figure 3a. (c) Interstadial salinity anomaly as the deviation from Figure 3a. (d) Sea ice cover (as % of the North Atlantic area) and annually averaged and seasonal AMOC maximum (Sv). (e) Decadal mean northward heat transport (PW) and decadally averaged AMOC strength through the sequence of individual D-O events. (f) Decadal mean maximum meridional northward salt transport (m^3/s) (~30°N) together with time-dependent salinity over the subtropical gyre and that in the polar halocline beneath the North Atlantic sea ice lid at 45°N latitude.

and salinity in the North Atlantic at 45°N latitude beneath the stadial sea ice lid. Once cold stadial conditions begin to develop, the latitudinal gradient of sea surface salinity continuously increases. Salinity of the subtropical gyre increases, and that of the halocline beneath the sea ice in the northern part of the basin decreases. Eventually, a critical salinity gradient is exceeded and a strong northward flux of salinity ensues. This causes the collapse of the salinity gradient which is accompanied by a reinvigoration of the AMOC and a transition to warm interstadial conditions. The sharp overshoot of AMOC strength (Figure 3f) that accompanies the reinvigoration of the overturning circulation at the onset of a single pulse is due to the contribution of enhanced northward salt transport to the densification of 45°N latitude Atlantic surface waters. This densification of Atlantic surface waters is expected based upon the dominance of the impact of the three practical salinity unit (psu) change in salinity on density that follows from the equation of state of sea water under near-freezing sea surface temperature (SST) conditions. The D-O oscillations in the model are therefore salt oscillations but a salt oscillation that does not involve any input of meltwater from the land-based ice sheets. In the recent analysis by *Zhang et al.* [2014] using CCSM3, the authors attempted to explain the processes involved in the instability of the AMOC during MOIS 3 as being associated with freshwater perturbations added to the North Atlantic. In our model this mechanism is irrelevant to the occurrence of oscillatory behavior, although it would be expected to cause the variability to be (perhaps significantly) modified. In CCSM3, since the AMOC is fundamentally stable under glacial conditions [*Vettoretti and Peltier*, 2013], the only way to generate oscillatory behavior is to force it through external means.

The connection of the Heinrich events with individual Bond cycles of D-O oscillation requires further discussion. In our version of the CESM1 model, as in our recent analyses of LGM climate using CCSM3 [*Vettoretti and Peltier*, 2013], there exist nonlinear thermal thresholds across which the state of the nonlinear coupled model changes very abruptly as the simulation proceeds from the "overheated" initial state (in which the oceans were assumed to have the modern thermal structure; see discussion in the supporting information) and climate cools. These thresholds are periods during which sharp reductions in North Atlantic surface air temperature occur which are accompanied by equally sharp expansions of sea ice cover. That such a threshold is crossed in the model just prior to the onset of the oscillatory behavior is demonstrated in Figure 2 (and in Figure S2 for the model based upon the use of the POP1 diffusivity profile) on which the

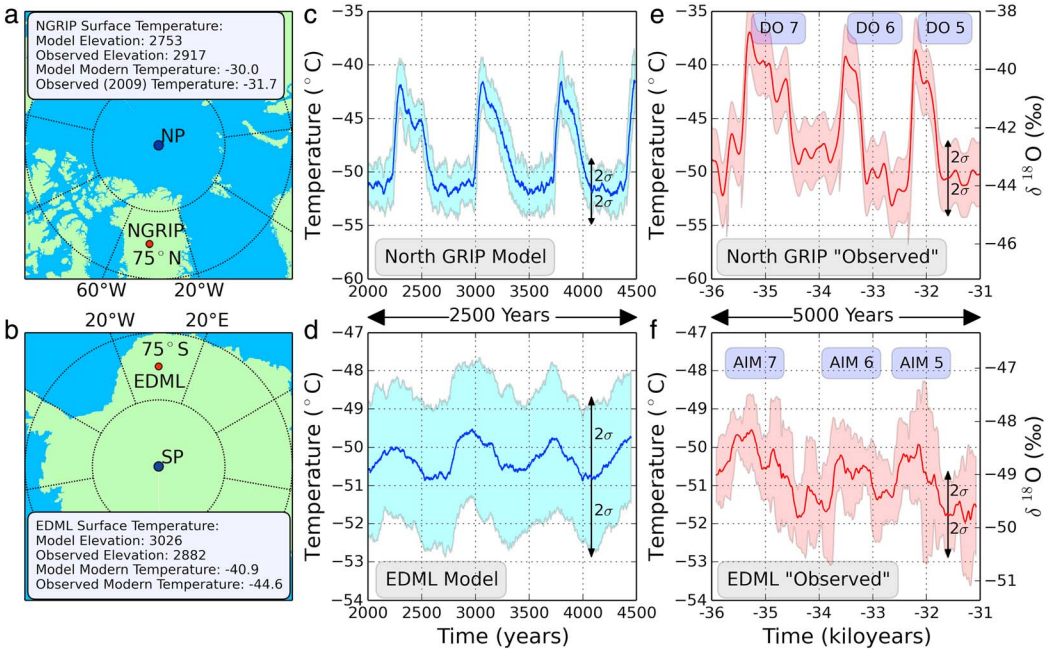

Figure 4. (a) NGRIP and (b) EDML locations. (c, d) Model-predicted temperature (°C) at NGRIP Summit-Greenland and EPICA Dronning Maud Land (EDML), Antarctica through three D-O cycles. (e, f) Ice core-inferred temperature variations based upon $\delta^{18}O$ (‰) at the NGRIP [*Huber et al.*, 2006] and EDML sites [*Stenni et al.*, 2010]. Two sigma error bars are estimated for all records shown.

threshold is denoted simply by "H." It is this thermal threshold, whose influence mimics the effect of a Heinrich event that is responsible for triggering the sequence of D-O oscillations in the model, thereby constituting the kick following which the salt oscillator oscillates. We have investigated the sensitivity of the oscillations induced by the thermal threshold effect to the addition of explicit freshwater forcing applied to the Ruddiman (ice-rafted debris) Belt of the North Atlantic (not shown) and demonstrated that there is no significant effect on the oscillatory behavior thereafter produced.

4. The Bipolar Seesaw

Even the earliest comparative analyses of ice core-derived climate information from the Greenland and Antarctic ice sheets led to the recognition of a "bipolar seesaw" relationship between climate variability in the Northern and Southern Hemispheres [*Broecker*, 1998; *Blunier and Brook*, 2001; *Morgan et al.*, 2002; *Stocker and Johnsen*, 2003; *Barbante et al.*, 2006]. Given that we have produced an explicit model of the millennium time scale D-O oscillation in Greenland ice cores, we are in a position to test the ability of the model to properly account for this observed global characteristic. Clearly evident from Figure 2 is the fact that CESM1 is capturing this bipolar seesaw behavior as the maxima in the strength of North Atlantic Deep Water cell in the North Atlantic correspond to minima in the strength of the AABW cell in the southern ocean. In Figure S3 in the supporting information we further illustrate this behavior in terms of global SST behavior through a single D-O cycle.

The quality of the CESM1 representation of the bipolar seesaw is further established by a comparison between observationally inferred and model-predicted atmospheric temperature variations at the locations of the NGRIP and EDML (European Project for Ice Coring in Antarctica (EPICA) Dronning Maud Land) ice cores on Greenland and Antarctica, respectively [*Huber et al.*, 2006; *Stenni et al.*, 2010]. No previous model of the D-O oscillation has ever been shown to fully account for this further characterization of the bipolar behavior.

Our comparisons of model-predicted and ice core-inferred variations of atmospheric temperature are shown in Figure 4 which compares the results for the three D-O pulses from the model with low diapycnal diffusivity with three D-O pulses in the data from both locations. For NGRIP the peak-to-peak variations of temperature in both model predictions and ice core-derived inferences is approximately 10°C. At Dronning Maud Land the signal

strength is much reduced to approximately 1.5° peak to peak in both model and data [*Huber et al*., 2006; *Stenni et al*., 2010]. The model is therefore successful in passing this bipolar test of the salt oscillator mechanism.

5. Discussion

Our analyses of glacial climate, based upon use of two alternative models for the diapycnal diffusivity profile employed in the CESM1 model, demonstrate that under conditions of fixed continental ice sheet mass, the cold climate of this period should be characterized by almost periodic oscillations on the millennium time scale following an appropriate Heinrich event-like kick into cold stadial conditions. The fast time scale governing the onset of each pulse is associated with convective destabilization of the water column in the North Atlantic, whereas the slow time scale relaxation phase is controlled by slow sea ice readvance and northward ocean heat flux decrease and the associated reestablishment of the high salinity of the subtropical gyre and the low salinity of the high-latitude halocline.

Having identified the fundamental salt oscillator physics underlying the D-O oscillation, we are in a position to explore further outstanding issues concerning millennium time scale rapid climate change. Such issues include the detailed controls on the period of the "bare" D-O oscillation that exists in the absence of the expected feedbacks associated with ice sheet response. As interesting is the connection between this "bare" form of the oscillation and the millennial time scale variability that dominates during the deglaciation phase of the 100 kyr ice age cycle itself during which the continental ice sheets are rapidly disintegrating. Further inspection of Figure 1a during this period of time shows that the Bolling-Allerod (B-A) transition (that began at approximately 14,200 years before present) was also preceded by an intense Heinrich event (labeled H1 on the figure). This transition was accompanied by a strong release of meltwater from the continental ice sheets that is referred to as meltwater pulse 1A in the Barbados record of relative sea level history [*Peltier and Fairbanks*, 2006]. It is notable that the sequence of events that follow H1 in the Summit, Greenland, ice core record are of D-O oscillation form.

Acknowledgments

The research has relied upon computational resources provided to W.R.P. by the SciNet facility for high-performance computation of the University of Toronto through the Compute Canada resource allocation process. SciNet is a component of the Compute Canada HPC platform. The research of W.R.P. at Toronto is supported by NSERC Discovery grant A9627.

Noah Diffenbaugh thanks Brian Rose and one anonymous reviewer for their assistance in evaluating this paper.

References

Alley, R. B., S. Anandakrishnan, and P. Jung (2001), Stochastic resonance in the North Atlantic, *Paleoceanography*, *16*, 190–198, doi:10.1029/2000PA000518.

Andersen, K., et al. (2004), High resolution record of Northern Hemisphere climate extending into the last interglacial period, *Nature*, *431*, 147–151, doi:10.1038/nature02805.

Argus, D. F., W. R. Peltier, R. Drummond, and A. W. Moore (2014), The Antarctica component of postglacial rebound model ICE-6G_C (VM5a) based on GPS positioning, exposure age dating of ice thickness, and relative sea level histories, *Geophys. J. Int.*, *198*(1), 537–563, doi:10.1093/gji/ggu140.

Barbante, C., et al. (2006), EPICA Community Members. One-to-one coupling of glacial climate variability in Greenland and Antarctica, *Nature*, *444*, 195–198, doi:10.1038/nature05301.

Birchfield, G. E., and W. S. Broecker (1990), A salt oscillator in the glacial Atlantic? 2. A "scale analysis" model, *Paleoceanography*, *5*, 835–843, doi:10.1029/PA005i006p00835.

Blunier, T., and E. J. Brook (2001), Timing of millennial-scale climate change in Antarctica and Greenland during the last glacial period, *Science*, *291*, 109, doi:10.1126/science.291.5501.109.

Bond, G., W. Showers, M. Cheseby, R. Lotti, P. Almasi, P. de Menocal, P. Priore, H. Cullen, I. Hajdas, and G. Bonani (1997), A pervasive millennial scale cycle in North Atlantic and Holocene and glacial climates, *Science*, *278*, 1257–1266, doi:10.1126/science.278.5341.1257.

Brady, E. C., B. Otto-Bliesner, J. E. Kay, and N. Rosenbloom (2013), Sensitivity to glacial forcing in the CCSM4, *J. Clim.*, *26*, 1901–19, doi:10.1175/JCLI-D-11-00416.1.

Broecker, W. S. (1998), Paleocean circulation during the last deglaciation: A bipolar seesaw?, *Paleoceanography*, *13*, 119–121, doi:10.1029/97PA03707.

Broecker, W. S., G. Bond, M. Klas, G. Bonani, and W. Wolfli (1990), A salt oscillator in the North Atlantic? 1: The concept, *Paleoceanography*, *5*, 469–477, doi:10.1029/PA005i004p00469.

Danabasoglu, G., S. Bates, B. P. Briegleb, S. R. Jayne, M. Jochum, W. G. Large, S. Peacock, and S. G. Yeager (2012), The CCSM4 ocean component, *J. Clim.*, *25*, 1361–1389, doi:10.1175/JCLI-D-11-00091.1.

Dansgaard, W., S. J. Johnsen, H. B. Clausen, D. Dahl-Jensen, N. Gundestrup, and C. U. Hammer (1984), North Atlantic climate oscillations revealed by deep Greenland ice-cores, in *Climate Processes and Climate Sensitivity*, *Geophys. Monogr. Ser.*, vol. 29, edited by J. E. Hansen and T. Takehashi, pp. 288–298, AGU, Washington, D. C.

Dansgaard, W., et al. (1993), Evidence for general instability of past climate from a 250 kyr ice-core record, *Nature*, *264*, 218–220, doi:10.1038/364218a0.

Dokken, T. M., K. H. Nisancioglu, C. Li, D. S. Battisti, and C. Kissel (2013), Dansgaard-Oeschger cycles: Interactions between ocean and sea ice intrinsic to the Nordic Seas, *Paleoceanography*, *28*, 491–502, doi:10.1002/palo.20042.

Ganopolski, A., and S. Rahmstorf (2002), Abrupt climate change due to stochastic resonance, *Phys. Rev. Lett.*, *88*(3), doi:10.1103/PhysRevLett.88.038501.

Gent, P. R., et al. (2011), The Community Climate System Model version 4, *J. Clim.*, *24*, 4973–4991, doi:10.1175/2011JCLI4083.1.

Griffiths, S. D., and W. R. Peltier (2009), Modeling of polar ocean tides at the Last Glacial Maximum: Amplification, sensitivity and climatological implications, *J. Clim.*, *22*, 2905–2924, doi:10.1175/2008JCLI2540.1.

Heinrich, H. (1988), Origin and consequences of cyclic ice rafting in the northeast North Atlantic ocean during the past 130,000 years, *Quat. Res.*, *29*, 142–153.

Hemming, S. R. (2004), Heinrich events: Massive late Pleistocene detritus layers of the North Atlantic and their global climate imprint, *Rev. Geophys.*, *42*, RG1005, doi:10.1029/2003RG000128.

Huber, C., M. Leuenberger, R. Spahni, J. Flückiger, J. Schwander, T. F. Stocker, S. Johnsen, A. Landais, and J. Jouzel (2006), Isotope calibrated Greenland temperature record over Marine Isotope Stage 3 and its relation to CH4, *Earth Planet. Sci. Lett.*, *243*, 504–519, doi:10.1016/j.epsl.2006.01.002.

Marsden, S. E., and M. McCracken (1976), *The Hopf Bifurcation and Its Applications*, Springer-Verlag, New York.

McManus, J. F., R. Francois, J.-M. Gherardi, L. D. Keigwin, and S. Brown-Leger (2004), Collapse and rapid resumption of Atlantic meridional circulation linked to deglacial climate changes, *Nature*, *428*, 834–837, doi:10.1038/nature02494.

Morgan, V., M. Delmotte, T. van Ommen, J. Jouzel, J. Chappellaz, S. Woon, V. Masson-Delmotte, and D. Raynaud (2002), Relative timing of deglacial climate events in Antarctica and Greenland, *Science*, *297*, 1862–1864, doi:10.1126/science.1074257.

Munk, W. H. (1966), Abyssal recipes, *Deep Sea Res.*, *113*, 207–230.

Munk, W. H., and C. Wunsch (1998), Abyssal recipes II: Energetics of tidal and wind mixing, *Deep Sea Res.*, *45*, 1977–2010.

Peltier, W. R., and R. G. Fairbanks (2006), Global glacial ice volume and Last Glacial Maximum duration from an extended Barbados sea level record, *Quat. Sci. Rev.*, *25*, 3322–3337, doi:10.1016/j.quascirev.2006.04.010.

Peltier, W. R., D. F. Argus, and R. Drummond (2014), Space geodesy constrains ice-age terminal deglaciation: The ICE-6G (VM5a) model, *J. Geophys. Res. Solid Earth*, doi:10.1002/2014GL061413.

Rose, B. E. J., D. Ferreira, and J. Marshall (2013), The role of oceans and sea ice in abrupt transitions between multiple climate states, *J. Clim.*, *26*, 2862–2879, doi:10.1175/JCLI-D-12-00175.1.

Sakai, K., and W. R. Peltier (1996), A multi-basin reduced model of the global Thermohaline circulation: Paleoceanographic analyses of the origins of ice-age climate variability, *J. Geophys. Res.*, *101*, 22,535–2561, doi:10.1029/96JC00539.

Sakai, K., and W. R. Peltier (1997), Dansgaard-Oeschger oscillations in a coupled atmosphere–ocean climate model, *J. Clim.*, *10*, 949–970, doi:10.1175/1520-0442(1997)010<0949:DOOIAC>2.0.CO;2.

Sakai, K., and W. R. Peltier (1999), A dynamical systems model of the Dansgaard-Oeschger oscillation and the origin of the Bond cycle, *J. Clim.*, *12*, 2238–2255, doi:10.1175/1520-0442(1999)012<2238:ADSMOT>2.0.CO;2.

Sakai, K., and W. R. Peltier (2001), The influence of deep ocean diffusivity on the temporal variability of the thermohaline circulation, in *The Oceans and Rapid Climate Change: Past, Present and Future*, *Geophys. Monogr. Ser.*, vol. 126, edited by D. Seidov and M. Maslin, pp. 227–242, AGU, Washington, D. C.

Singh, H. A., D. S. Battisti, and C. M. Bitz (2014), A heuristic model of the Dansgaard-Oeschger cycles: Description, results, and sensitivity studies, *J. Clim.*, *27*, 4337–4358, doi:10.1175/JCLI-D-12-00672.1.

Stenni, B., et al. (2010), The deuterium excess records of EPICA Dome C and Dronning Maud Land ice cores (East Antarctica), *Quat. Sci. Rev.*, *29*, 146–159, doi:10.1016/j.quascirev.2009.10.009.

Stocker, T. F., and S. J. Johnsen (2003), A minimum thermodynamic model for the bipolar seesaw, *Paleoceanography*, *18*(4), 1087, doi:10.1029/2003PA000920

Timmermann, A., M. Schulz, H. Gildor, and E. Tziperman (2003), Coherent resonant millennial-scale climate transitions triggered by massive meltwater pulses, *J. Clim.*, *16*(15), 2569–2585, doi:10.1175/1520-0442(2003)016<2569:CRMCOT>2.0.CO;2.

Van der Pol, B., and J. Van der Mark (1928), The heartbeat considered as a relaxation oscillation, and an electrical model of the heart, *London, Edinburgh, Dublin Philos. Mag. J. Sci.*, *6*(38), 763–775.

Vettoretti, G., and W. R. Peltier (2013), Last Glacial Maximum ice-sheet impacts on North Atlantic climate variability, *Geophys. Res. Lett.*, *40*, 6378–6383, doi:10.1002/2013GL058486.

Waelbroeck, L., L. Labeyrie, E. Michel, J. C. Duplessy, J. F. McManus, K. Lambeck, E. Balbon, and M. Labracherie (2002), Sea level and deep water temperature changes derived from benthic foraminifera isotopic records, *Quat. Sci. Rev.*, *21*, 295–305, doi:10.1016/S0277-3791(01)00101-9.

Waterhouse, A. F., et al. (2014), Global patterns of diapycnal mixing from measurements of the turbulent dissipation rate, *J. Phys. Oceanogr.*, *44*, 1854–1872, doi:10.1175/JPO-D-13-0104.1.

Weber, S. L., et al. (2007), The modern and glacial overturning circulation in the Atlantic ocean in PMIP coupled model simulations, *Clim. Past*, *3*, 51–64.

Zhang, X., G. Lohmann, G. Knorr, and X. Xu (2013), Different ocean states and transient characteristics in Last Glacial Maximum simulations and implications for deglaciation, *Clim. Past*, *9*, 2319–2333, doi:10.5194/cp-9-2319-2013.

Zhang, X., M. Prange, U. Merkel, and M. Schulz (2014), Instability of the Atlantic overturning circulation during Marine Isotope Stage 3, *Geophys. Res. Lett.*, *41*, 4285–4293, doi:10.1002/2014GL060321.